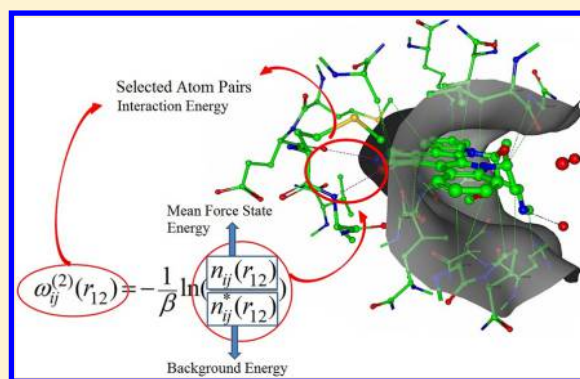# Development of the Knowledge-Based and Empirical Combined Scoring Algorithm (KECSA) To Score Protein−Ligand Interactions

Zheng Zheng and Kenneth M. Merz, Jr.*

Department of Chemistry and the Quantum Theory Project, 2328 New Physics Building, P.O. Box 118435, University of Florida, Gainesville, Florida 32611-8435, United States

Ⓢ *Supporting Information*

ABSTRACT: We describe a novel knowledge-based protein−ligand scoring function that employs a new definition for the reference state, allowing us to relate a statistical potential to a Lennard-Jones (LJ) potential. In this way, the LJ potential parameters were generated from protein−ligand complex structural data contained in the Protein Databank (PDB). Forty-nine (49) types of atomic pairwise interactions were derived using this method, which we call the knowledge-based and empirical combined scoring algorithm (KECSA). Two validation benchmarks were introduced to test the performance of KECSA. The first validation benchmark included two test sets that address the training set and enthalpy/entropy of KECSA. The second validation benchmark suite included two large-scale and five small-scale test sets, to compare the reproducibility of KECSA, with respect to two empirical score functions previously developed in our laboratory (LISA and LISA+), as well as to other well-known scoring methods. Validation results illustrate that KECSA shows improved performance in all test sets when compared with other scoring methods, especially in its ability to minimize the root mean square error (RMSE). LISA and LISA+ displayed similar performance using the correlation coefficient and Kendall τ as the metric of quality for some of the small test sets. Further pathways for improvement are discussed for which would allow KECSA to be more sensitive to subtle changes in ligand structure.

Selected Atom Pairs
Interaction Energy

Mean Force State
Energy

$$\omega_{ij}^{(2)}(r_{12}) = -\frac{1}{\beta} \ln\left(\frac{n_{ij}(r_{12})}{n_{ij}^*(r_{12})}\right)$$

Background Energy

INTRODUCTION

Knowledge-based protein−ligand scoring functions,[1−18] building on the idea of the potential of mean force (PMF),[19] are derived from structural information regarding protein−ligand complexes. Their pairwise interaction parameters are directly converted from the frequency of occurrence of given atom pairs contained in a large database of complexes. The concept of the potential of mean force can be illustrated by a simple fluid system of N particles whose positions are $r_1 \cdots r_N$. The average potential $\omega^{(n)}(r_1 \cdots r_N)$ is expressed as

$$\omega^{(n)}(r_1 \cdots r_n) = -\frac{1}{\beta} \ln(g^{(n)}(r_1 \cdots r_n)) \tag{1}$$

where $g^{(n)}$ is called a correlation function. $\beta = 1/k_B T$, where k_B is the Boltzmann constant and T is the system temperature. Hence, the mean potential of the system with N particles is strictly the potential that gives the average force over all the configurations of the $n + 1, ..., N$ particles acting on a particle at any fixed configuration, keeping the $1, ..., n$ particles fixed. The mean potential can be described as follows:

$$-\nabla_j \omega^{(n)} = \frac{\int \cdots \int e^{-\beta U} (\nabla_j U) \, dr_{n+1} \cdots dr_N}{\int \cdots \int e^{-\beta U} \, dr_{n+1} \cdots dr_N} \qquad j = 1, 2, ..., n \tag{2}$$

where U is the total potential energy of the system. Described by Sippl and others,[1−5] the average potential is expressed as eq 3 for the special case of a system with an observed particle number of $n = 2$, as is the case herein (pairwise atoms from the protein and ligand).

$$\omega_{ij}^{(2)}(r_{12}) = -\frac{1}{\beta} \ln(g^{(2)}(r_{12})) = -\frac{1}{\beta} \ln\left(\frac{\rho_{ij}(r_{12})}{\rho_{ij}^*(r_{12})}\right) \tag{3}$$

where $g^{(2)}(r)$ is the pair distribution function, $\rho_{ij}(r)$ is the number density for the atom pairs of types i and j observed in the known protein structures and $\rho_{ij}^*(r)$ is the number density of the corresponding pair in a reference state. In order to obtain the pure interaction potential between atoms, a reference state is required to remove the contribution of the ideal-gas state potential. So, in the reference state, the system of particles is like an ideal-gas state defined by fundamental statistical mechanics, in which particles would be evenly distributed in the binding site. Eq 3 also can be expressed as
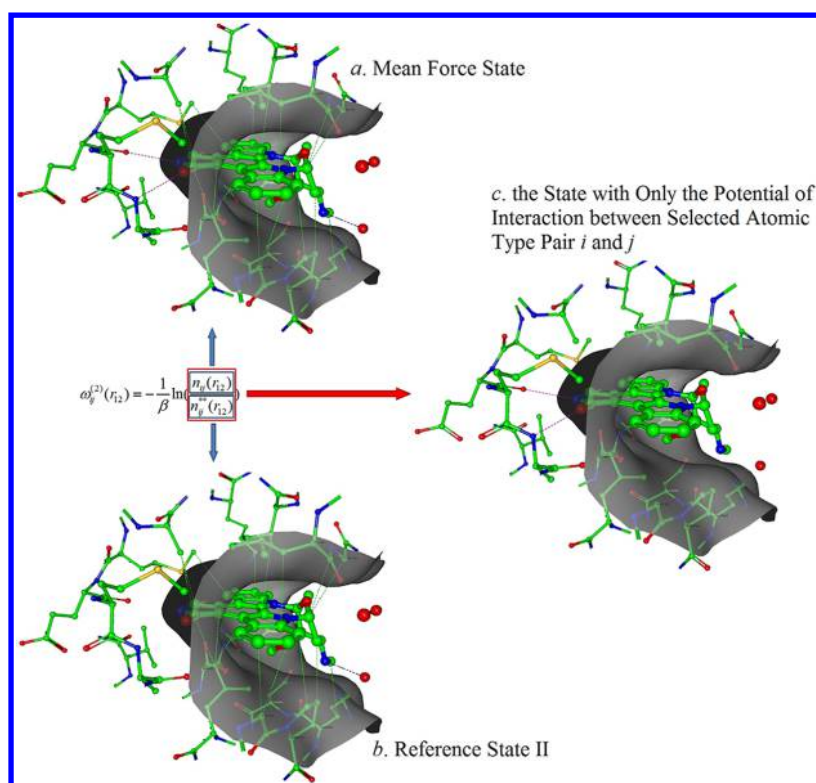
Figure 1. A protein−ligand structural illustration (using PDBID 1xbc) of how the KECSA statistical potential is modeled. The protein binding site is shown as a gray surface with the ligand located within the binding site surrounded by protein residues which it makes contact with. The pink dashed lines indicate interactions between certain atom pair types i and j, (i.e., carbonyl oxygen with amine nitrogens in this example) which are defined as "selected interactions" in this manuscript. Green dashed lines indicate all other noncovalent interactions between the protein and ligand atoms in the binding pocket, defined as "background interactions". (a) In the mean force state, the system is filled with all types of interactions. (b) The reference state II contains all the background interactions. (c) Removing all the background interactions from the total interactions results in a state with only the selected interactions for each i and j combination.

$$\omega_{ij}^{(2)}(r_{12}) = -\frac{1}{\beta}\ln(g^{(2)}(r_{12})) = -\frac{1}{\beta}\ln\left(\frac{n_{ij}(r_{12})}{n_{ij}^*(r_{12})}\right) \qquad (4)$$

where $n_{ij}(r)$ and $n_{ij}^*(r)$ are numbers of atom pairs of type i and j, respectively, at distance r for the observed structures and the reference state.

In potential of mean force methods, the number of the corresponding pairs in the reference state cannot be exactly obtained for protein−ligand systems due to the effects of connectivity, excluded volume, composition, etc.[6] Therefore, the pairwise interaction potential cannot be accurately calculated. Nonetheless, this idea of PMF scoring has advantages over empirical scoring, because it directly relates pairwise interaction to structural data, instead of fitting to known binding affinity data. In addition, the PMF is more efficient than force field scoring, because of the avoidance of higher-expense computations. Our intent is to introduce a new concept of the reference state, in order to relate the statistical potential to atomic pairwise interaction potential. Hence, the atomic pairwise interaction model can be parametrized exclusively from structural data, instead of binding data or quantum calculations.

METHODS AND RESULTS

The construction of traditional statistical potentials starts with the collection of structural information from large numbers of protein−ligand complexes, in order to simulate a "mean force" state in which the protein−ligand atomic pairwise radial distribution arises from all possible interactions in the binding site. Various reference states have been designed to remove the noninteracting energy from the mean force state, in order to correlate the pairwise radial distribution to the interaction potential between selected atoms of a specific atom type i,j with all other atoms in the protein−ligand binding site.

Our goal is to equate the statistical potential to the Lennard-Jones (LJ) potential for each pairwise interaction. However, the LJ potential reflects pairwise interactions between two types of atoms, while a statistical potential is an average potential contributed by all atoms within the binding region. In this case, when trying to equate the statistical potential to a pairwise interaction potential, we must remove all interactions except the pairwise interaction between atoms of type i,j in the binding region by defining a new reference state (denominator) in the PMF model. Unlike the traditional reference state, in which the selected atom pairs i,j are at an infinite separation where the interaction energy is zero (as in the ideal gas state), within this new reference state (which we will call reference state II), a system of particles is under an average force contributed by all atoms in the binding region excluding the interaction force between the selected atom pairs i,j. In other words, the only difference between the mean force state and reference state II is that the latter state does not contain the pairwise interaction potential between the selected atoms of type i and j. Figure 1 provides a graphic illustration of the KECSA statistical potential model.
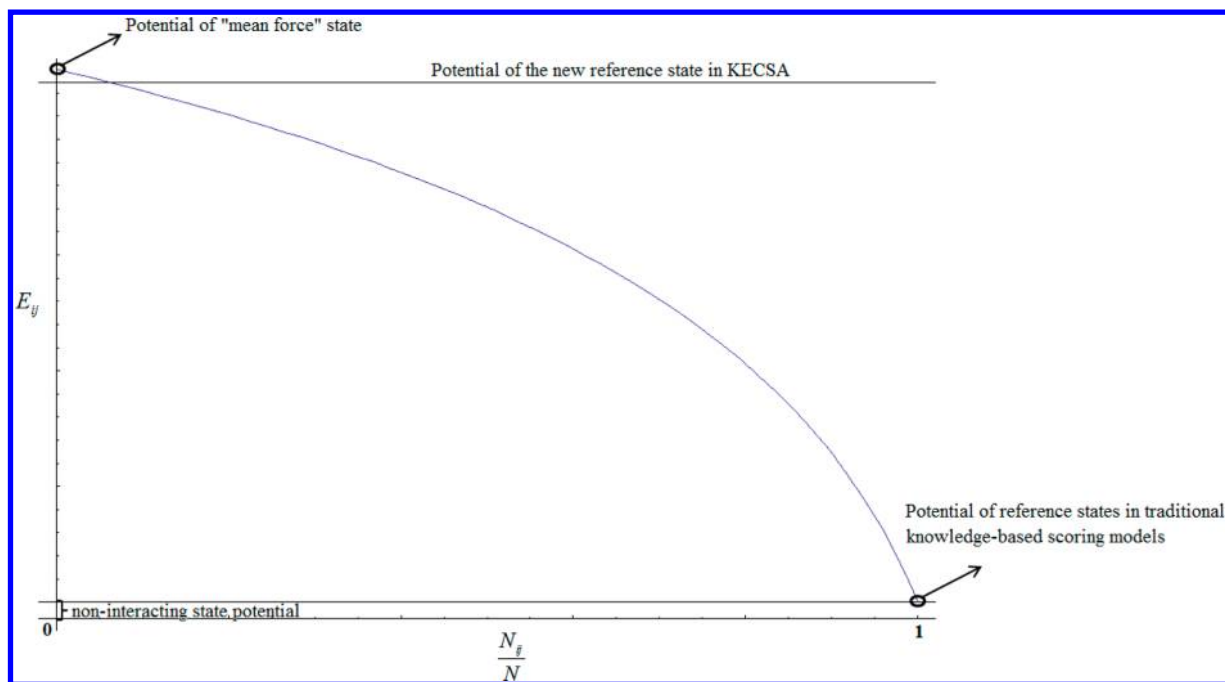
Figure 2. Ratio of the observed atom pairs to the total interacting atom pairs N_{ij}/N versus the new reference state II potential.

When equated to the LJ potential, the statistical potential can be expressed as

$$E_{ij}(r) = -RT \ln\left[\frac{n_{ij}(r)}{n_{ij}^{**}(r)}\right]$$

$$= RT(\ln[n_{ij}^{**}(r)] - \ln[n_{ij}(r)])$$

$$= \frac{-1}{\left(\frac{\beta}{\alpha}\right)^{\alpha/(\alpha-\beta)} - \left(\frac{\beta}{\alpha}\right)^{\beta/(\alpha-\beta)}} \varepsilon\left[\left(\frac{\sigma}{r_{ij}}\right)^{\alpha} - \left(\frac{\sigma}{r_{ij}}\right)^{\beta}\right] \tag{5}$$

where σ is the distance at which the interparticle potential is zero and ε is the well depth. The exponents for the repulsive term and the attractive term are α and β, respectively. We derive the exponents instead of assigning "typical" exponent values (i.e., 12−6), because (1) the repulsive and attractive forces change with different types of pairwise interactions and (2) $E_{ij}(r)$ in eq 5 includes both van der Waals and electrostatic interactions, which means the LJ-potential formula on the right-hand side of eq 5 accounts for two components:

$$\frac{-1}{\left(\frac{\beta}{\alpha}\right)^{\alpha/(\alpha-\beta)} - \left(\frac{\beta}{\alpha}\right)^{\beta/(\alpha-\beta)}} \varepsilon\left[\left(\frac{\sigma}{r_{ij}}\right)^{\alpha} - \left(\frac{\sigma}{r_{ij}}\right)^{\beta}\right]$$

$$\approx 4\varepsilon_0\left[\left(\frac{\sigma_0}{r_{ij}}\right)^{12} - \left(\frac{\sigma_0}{r_{ij}}\right)^{6}\right] + \frac{q_1 q_2}{\varepsilon_1 r_{ij}} \tag{6}$$

The reason we use the LJ formula on the left-hand side of eq 6 instead of partitioning them into van der Waals and electrostatic potentials is that the LJ potential reaches 0 at σ and R, while reaching its minimum value when r is $((\alpha/\beta)^{1/(\alpha-\beta)}\sigma)$. Based on these properties, equations can be derived in order to determine the unknown parameters.

In eq 5, $n_{ij}^{**}(r)$ and $n_{ij}(r)$ are the number of protein−ligand atomic pairwise interactions in the bin $(r, r + \Delta r)$, with the

volume $4\pi r^a \Delta r$ in reference state II and in the training set that mimics the mean force state, respectively. Δr is defined as 0.005 Å. We introduce a to-be-determined parameter a for the shell volume because of the inaccessible volume present in protein−ligand systems, and because of the deviation of $n_{ij}(r)$ in the training set from the "perfect" pairwise number. Hence, the expectation is that parameter a will adopt values other than 2.

The central issue in the KECSA model construction is to build up the radial distribution function of the selected atom pairs in reference state II. A way in which to do this is to measure the similarity of the reference state II with two known states: the mean force state, and ideal gas state. Then build the radial distribution function with information collected from these two states. In reference state II, the radial distribution of a certain atom pair i,j is associated with a certain "background interaction", which is related to the total number of selected atom pairs N_{ij}. Because the background interaction potential contains all atom pairwise interactions in the binding site excluding the "selected interactions" between atom pairs i,j, the difference in energy between the mean force state and reference state II for each atom pair type depends on the total number of selected atom pairs N_{ij} and the total number of atom pairwise interactions N found in the binding site. The background interaction energy approaches the mean force state energy as the ratio N_{ij}/N becomes smaller, while the energy difference increases when the ratio N_{ij}/N becomes larger. Hence, we decided to make the "background interaction" potential, as well as the radial distribution function, a function of the ratio N_{ij}/N. The modeling of the atom pairwise number distribution function in reference state II starts from the two extreme situations for N_{ij}/N:

(1) When N_{ij} approaches zero $(N_{ij} \rightarrow 0)$, the background energy ≈ the "mean force" state energy, resulting in $n_{ij}^{**}(r) \approx n_{ij}(r)$.

(2) When N_{ij} approaches N $(N_{ij} \rightarrow N)$, the background energy is approximately equal to the ideal-gas energy,

resulting in $n_{ij}^{**}(r)$ resembling an ideal gas state radial distribution.

The radial distribution function for an ideal gas state is defined as $(N_{ij}/(V4\pi r^a \Delta r))$, implying that the number of the selected atom pairs i,j is evenly distributed in the binding site, which has an average volume V. The V value of the protein–ligand binding site is given as $(4/((a+1)\pi R^{a+1}))$, with the same to-be-determined parameter a as introduced above. Hence, the two extreme situations for reference state II can be defined as

$$n_{ij}^{**}(r) = \left(\frac{N_{ij}}{V}4\pi r^a \Delta r\right) \qquad N_{ij} \to N \tag{7}$$

$$n_{ij}^{**}(r) = n_{ij}(r) \qquad N_{ij} \to 0 \tag{8}$$

At a certain distance r, $n_{ij}^{**}(r)$ is a function of N_{ij}/N, with a range of values from $(N_{ij}/V)4\pi r^a \Delta r$ to $n_{ij}(r)$. In addition, with N_{ij} tending toward 0 or N, the reference state II would be more similar to the mean force state or the ideal gas state, respectively. Hence, $n_{ij}^{**}(r)$ is defined as a weighted combination of both the ideal gas state and the mean force state radial distribution functions. Because of the fact that the integral of $n_{ij}^{**}(r)$ from 0 to R (cutoff distance where the atomic interaction is regarded as zero) is N_{ij}, a linear combination (eq 9) of the weighted radial distribution functions for both the ideal gas and mean force state meets all the necessary conditions:

$$n_{ij}^{**}(r) = \left(\frac{N_{ij}}{V}4\pi r^a \Delta r\right)\frac{N_{ij}}{N} + (n_{ij}(r))\left(1 - \frac{N_{ij}}{N}\right) \tag{9}$$

In this way, the new reference state is designed as a state intermediate between the ideal gas and the mean force state. At a certain distance between the atom pairs of type i,j, the total energy of reference state II ($E_{ij}^{**}(r)$), or the background interaction energy, is

$$E_{ij}^{**}(r) = -\frac{1}{\beta}\ln(n_{ij}^{**}(r))$$
$$= -\frac{1}{\beta}\ln\left[\left(\frac{N_{ij}}{V}4\pi r^a \Delta r\right)\frac{N_{ij}}{N} + (n_{ij}(r))\left(1 - \frac{N_{ij}}{N}\right)\right] \tag{10}$$

A plot illustrating the relationship between the number fraction (N_{ij}/N) and the new reference state potential $E_{ij}^{**}(r)$ is shown in Figure 2, to better illustrate the differences in energy between the different states.

Combining eqs 5 and 9, we obtain

$$\ln\left[\left(\frac{N_{ij}}{V}4\pi r^a \Delta r\right)\frac{N_{ij}}{N} + (n_{ij}(r))\left(1 - \frac{N_{ij}}{N}\right)\right] - \ln(n_{ij}(r))$$
$$= \frac{-1}{\left(\frac{\beta}{\alpha}\right)^{\alpha/(\alpha-\beta)} - \left(\frac{\beta}{\alpha}\right)^{\beta/(\alpha-\beta)}}\left(\frac{\varepsilon}{RT}\right)\left[\left(\frac{\sigma}{r_{ij}}\right)^\alpha - \left(\frac{\sigma}{r_{ij}}\right)^\beta\right] \tag{11}$$

Using $V = (4/(a+1))\pi R^{a+1}$, and using the fact that the LJ potential is zero at $r_{ij} = \sigma$ and at $r_{ij} = R$, we arrive at

$$\ln\left[\frac{N_{ij}}{N}\left(\frac{N_{ij}(a+1)\sigma^a \Delta r}{R^{a+1}n_{ij}(\sigma)}\right) + \left(1 - \frac{N_{ij}}{N}\right)\right] = 0 \tag{12}$$

and

$$\ln\left[\frac{N_{ij}}{N}\left(\frac{N_{ij}(a+1)R^a \Delta r}{R^{a+1}n_{ij}(R)}\right) + \left(1 - \frac{N_{ij}}{N}\right)\right] = 0 \tag{13}$$

In addition, the LJ potential reaches its minimum value when r is $\sigma(\alpha/\beta)^{(1/(\alpha-\beta))}$. Therefore, the first derivative (D) of the statistical energy term, with respect to r, is zero at $r = \sigma(\alpha/\beta)^{(1/(\alpha-\beta))}$.

$$D\left[-\frac{1}{RT}\ln\left(\frac{n_{ij}(r)}{n_{ij}^{**}(r)}\right), r = \sigma\left(\frac{\alpha}{\beta}\right)^{1/(\alpha-\beta)}\right] = 0 \tag{14}$$

To simplify the resultant expressions, the factor $(\alpha/\beta)^{(1/(\alpha-\beta))}$ is given as η:

$$D\left[-\frac{1}{RT}\ln\left(\frac{n_{ij}(r)}{n_{ij}^{**}(r)}\right), r = \eta\sigma\right]$$
$$= \frac{a\frac{N_{ij}}{N}\left(\frac{N_{ij}(a+1)(\eta\sigma)^{a-1}\Delta r}{R^{a+1}n_{ij}(\eta\sigma)}\right) - \frac{N_{ij}}{N}\left(\frac{N_{ij}(a+1)(\eta\sigma)^{a-1}\Delta r}{R^{a+1}n_{ij}^2(\eta\sigma)}\right)D(n_{ij}(\eta\sigma))}{\frac{N_{ij}}{N}\left(\frac{N_{ij}(a+1)(\eta\sigma)^a \Delta r}{R^{a+1}n_{ij}(\eta\sigma)}\right) + \left(1 - \frac{N_{ij}}{N}\right)}$$
$$= 0 \tag{15}$$

Simplifying eqs 12, 13, and 15 yields

$$N_{ij}(a+1)\sigma^a \Delta r = R^{a+1}n_{ij}(\sigma) \tag{16}$$

$$N_{ij}(a+1)R^a \Delta r = R^{a+1}n_{ij}(R) \tag{17}$$

and

$$an_{ij}(\eta\sigma) = D(n_{ij}(\eta\sigma)) \tag{18}$$

Although we do not know the values of α and β yet, we do know that the value of η is unique for each combination of α and β. Table 1 in the Supporting Information lists all η values for each integer combination of α and β from 2 to 1 to 15–14. Different η values will be chosen for every pairwise interaction, to satisfy the well depth distance at $\eta\sigma$ (e.g., $(\alpha/\beta)^{(1/(\alpha-\beta))}\sigma$ is $2^{1/6}\sigma$ or r_{ij}^* (well depth at the minimum) for the 12–6 potential).

In order to determine the values of a, σ, and η within eqs 16–18, we still need to determine the value of R, the cutoff distance. We introduce a nonlinear programming method to find a reasonable R for each pairwise interaction type instead of assigning a fixed R value. Ideally, R should be as large as possible since the LJ potential approaches 0 when the distance approaches infinity. Meanwhile, for any r between σ and R, the potential value is below 0. Here, we use the following inequality constraint in our nonlinear programming approach:

$$\frac{1}{RT}\ln\left[\frac{N_{ij}}{N}\left(\frac{N_{ij}(a+1)r^a \Delta r}{R^{a+1}n_{ij}(r)}\right) + \left(1 - \frac{N_{ij}}{N}\right)\right] < 0$$
$$\sigma < r < R \tag{19}$$

which can be simplified as

$$N_{ij}(a+1)r^a \Delta r < R^{a+1}n_{ij}(r) \qquad \sigma < r < R \tag{20}$$

With the goal of maximizing the value of R, coupled with the three constraint equations (eqs 16–18) and an inequality constraint (eq 20), a, σ, and η can be determined. The values of

1076

dx.doi.org/10.1021/ci300619x | J. Chem. Inf. Model. 2013, 53, 1073–1083

η obtained in this way can then be compared with the η values in Table 1 in the Supporting Information, in order to determine the closest α and β pair. Inserting these values into eq 11, we can calculate all of the corresponding ε values.

One important issue in the parametrization of KECSA is that the LJ potential parameters for each type of pairwise interaction should be independent of the other types of interactions, instead of being dependent on N_{ij}/N. Derivation of a, σ, α, β, and R comes from eqs 16−18 and eq 20, none of which contains the total interaction number (N). This indicates that, for each type of pairwise interaction, the average volume ($(4/a + 1)\pi R^{a+1}$), the distances at which the LJ potential reaches zero and has a minimum (σ and $(\alpha/\beta)^{(1/(a-\beta))}\sigma$), the relative strength of the repulsive and attractive forces in the LJ potential (α and β), and the long-range cutoff distance (R) are independently derived in KECSA. The only issue lies in the derivation of the ε values from eq 11, where the probability of occurrence (N_{ij}/N) is included in the calculation. In order to avoid relative energies generated for each interaction type based on their probability of occurrence in protein−ligand binding sites, we used a normalized N_{ij}/N value for each interaction type. Thereby, the number fractions for all interaction types are identical.

In the present work, all pairwise interactions among 18 atom types (listed in Table 1) were examined, resulting in 49

Table 1. List of Selected Atom Types

atom type	description
C3	sp^3-hybridized carbon
C2	sp^2-hybridized carbon
Car	aromatic carbon
C1	sp-hybridized carbon
N4	positively charged nitrogen
Nam	amide nitrogen
N3	sp_3-hybridized nitrogen
Nar	nitrogen aromatic
N2	sp_2-hybridized nitrogen
Npl3	trigonal planar nitrogen
O3	sp^3-hybridized oxygen
O2	sp^2-hybridized oxygen
S	sulfur
P	phosphorus
F	fluorine
Cl	chlorine
Br	bromine
I	iodine

significant interaction types being identified. The remaining interaction types were abandoned or merged into similar interaction types, because of the paucity of data to which to fit, or because they are randomly distributed across the observed distance range. The chosen interaction types included 38 van der Waals interaction types and 11 hydrogen bonding interaction types. In this case, all interaction types share the same probability of occurrence ($(N_{ij}/N) = 1/49$) in protein−ligand binding sites. Eq 11 can be rewritten as follows in order to generate the ε values.

$$\ln\left[\left(\frac{N_{ij}}{V}4\pi r^a \Delta r\right)\frac{1}{49} + (n_{ij}(r))\left(1 - \frac{1}{49}\right)\right] - \ln[n_{ij}(r)]$$

$$= \frac{-1}{\left(\frac{\beta}{\alpha}\right)^{\alpha/(\alpha-\beta)} - \left(\frac{\beta}{\alpha}\right)^{\beta/(\alpha-\beta)}}\frac{\varepsilon}{RT}\left[\left(\frac{\sigma}{r_{ij}}\right)^\alpha - \left(\frac{\sigma}{r_{ij}}\right)^\beta\right]$$

(21)

All derived parameters are listed in Table 2.

With all of the enthalpy terms determined in the analytical manner described above, the entropy terms were then decided upon in an empirical manner. Structural information such as the number of rotatable bonds, number of double and aromatic bonds, molecular mass, counts of C/O/N atoms, buried surface area, etc. were collected for all ligands contained in the training set. The selection of the entropy terms is based on their contribution to our linear regression model, whose 95% confidence interval should not include 0. (See Table 3.) Finally, nine entropy terms were selected: number of rotatable bonds in the ligand, the molecular mass of the ligand, number of aromatic bonds in the ligand, number of oxygen atoms in the ligand, number of nitrogen atoms in the ligand, the nonpolar buried surface area, total buried surface area, the ratio of the nonpolar buried surface and total ligand surface area and, finally, the ratio of the total buried surface area and the total ligand surface area. The PDBbind v2010 dataset[21,22] including 5054 protein−ligand complexes is chosen as the training set for the parametrization of the enthalpy terms. We chose 1982 protein−ligand complexes found in the PDBbind v2011 refined dataset as the training set for the selection and parametrization of the entropy terms.

■ MODEL VALIDATION AND DISCUSSION

I. Validation To Detect Overfitting and Ligand-Size Dependence. Several validation benchmarks were introduced to test the performance of KECSA. The first benchmark included two test sets in order to examine the dependence of KECSA on the training set. Because the entropy term was obtained by fitting to experimental binding free energies, care was taken to ensure that the resultant model was not overfit. First, a leave-one-out cross validation was used against the training set, which includes 1982 protein−ligand complexes used in the KECSA entropy term parametrization. Comparisons of the Pearson correlation coefficient (r), the root-mean-square error (RMSE), and the Kendall parameter (τ) between the training set and the leave-one-out cross validation are shown in Table 4. The three statistical measures all showed small differences between the training set and the leave-one-out prediction, indicating that the KECSA entropy model was properly built.

Second, we introduced a test set including 1934 protein−ligand complexes chosen from the PDBbind v2011 dataset, with no overlap with the training set used above. From the total of 6051 protein−ligand complexes with binding affinity data in the PDBbind v2011 dataset, complexes for this test set were selected following four criteria:

(1) Crystal structures of all selected complexes had X-ray resolutions ≤2.5 Å.

(2) Only complexes with pK_i or pK_d values distributed between 2 to 8 were selected, mimicking what might be found in a virtual screening database or a pharmaceutically relevant ligand database.

Table 2. Parameters for All 49 Pairwise Potentials

interaction type	C2C2	C2Car	C2N2	C2N3	C2N4	C2Nam	C2Nar	C2Npl3	C2O2	C2O3
σ	4.145	3.630	3.450	3.285	3.215	3.505	3.575	3.505	3.370	3.135
a	3.375	2.224	3.085	2.810	3.089	4.296	2.662	2.273	3.298	2.992
R	5.900	6.535	4.755	4.220	4.235	4.265	5.390	6.485	4.430	5.345
ε	0.091	0.041	0.388	0.035	0.133	1.003	0.296	0.769	1.735	0.071
LJ model	12−5	11−1	10−9	12−8	14−12	15−6	12−11	15−14	12−11	13−4
interaction type	C2S	C3C2	C3C3	C3Car	C3N2	C3N3	C3N4	C3Nam	C3Nar	C3Npl3
σ	4.350	3.940	4.290	3.850	3.580	3.650	4.570	4.470	3.455	3.815
a	2.505	3.049	2.759	2.237	2.404	1.759	2.988	3.581	2.990	2.347
R	6.425	6.210	6.840	6.775	6.130	6.945	6.850	6.165	5.435	6.160
ε	0.387	0.085	0.364	0.454	0.053	0.123	0.022	0.071	0.067	0.129
LJ model	12−11	14−3	5−4	5−3	15−9	13−12	12−7	12−7	12−9	4−3
interaction type	C3O2	C3O3	C3S	CarCar	CarN2	CarN3	CarN4	CarNam	CarNar	CarNpl3
σ	3.200	3.325	3.940	3.700	3.600	3.700	4.360	3.720	3.565	3.665
a	2.742	3.164	1.965	1.898	2.079	2.032	1.089	3.655	1.389	1.736
R	4.515	5.650	6.630	6.855	6.440	6.845	6.980	6.030	6.865	6.675
ε	0.343	0.038	0.016	0.249	0.013	0.005	0.056	0.279	0.206	0.016
LJ model	9−6	13−7	14−1	4−3	11−1	8−1	9−5	14−13	15−14	15−6
interaction type	CarO2	CarO3	CarS	N2O2HB	N2O3HB	N3O2HB	N3O3HB	NamO2HB	NamO3HB	Npl3O2HB
σ	3.430	3.690	3.920	2.640	2.670	2.550	2.605	2.610	2.625	2.585
a	2.840	2.204	1.627	2.056	2.365	0.989	1.788	2.057	3.475	1.377
R	6.600	6.505	6.975	6.420	6.465	6.745	4.585	4.765	4.160	4.995
ε	0.120	0.030	0.050	0.062	0.036	0.196	0.217	1.700	0.172	0.219
LJ model	12−10	6−2	9−5	15−8	15−5	14−10	13−9	12−10	11−8	13−8
interaction type	Npl3O3HB	O2N2	O2Nam	O2Nar	O2O2	O3N2HB	O3O2HB	O3O2	O3O3HB	
σ	2.635	2.570	4.125	3.380	3.065	2.510	2.445	3.365	2.080	
a	1.899	2.397	2.784	2.292	2.767	1.345	1.998	3.250	2.408	
R	6.755	6.845	6.065	6.070	6.055	4.395	6.065	6.480	6.990	
ε	0.272	0.010	0.008	0.073	0.034	0.116	2.002	0.024	0.038	
LJ model	15−12	7−1	13−3	11−7	4−1	15−8	14−13	3−2	11−3	

Table 3. Entropy Parameters and Their 95% Confidence Intervals

	parameter	95% Confidence Interval	
		lower limit	upper limit
enthalpy	0.0928	0.0650	0.1206
number of rotatable bonds	0.0900	0.0601	0.1200
molecular mass	−0.0170	−0.0191	−0.0149
N_number	0.2455	0.1838	0.3072
O_number	0.3131	0.2528	0.3733
number of aromatic bonds	0.0359	0.0130	0.0588
nonpolar buried surface area	0.0152	0.0047	0.0257
total buried surface area	−0.0089	−0.0167	−0.0012
nonpolar buried surface area/total surface area	−4.1454	−6.9496	−1.3412
total buried surface area/total surface area	−6.2438	−8.1509	−4.3368

Table 4. Leave-One-Out Cross Validation of KECSA

	Pearson's r	RMSE (kcal/mol)	Kendall τ
training	0.601	2.20	0.442
leave-one-out calculation	0.594	2.22	0.437

(3) Only complexes with molecular weights (MWs) distributed from 80 to 800 were selected, to avoid ligand size-dependent prediction results.

(4) Complexes used in the KECSA entropy term training set were excluded.

The second test set was used to verify the robustness of KECSA against an external dataset, as well as investigating the contributions of the enthalpy and entropy terms in KECSA's binding affinity prediction. In addition, because the entropy term in KECSA was modeled as a linear combination of several ligand properties including ligand size/mass information this test demonstrated that KECSA was not ligand size-dependent. We split the KECSA scoring function and used both LJ potential and entropy terms for binding affinity prediction, and then we compared it with the full KECSA scoring function. We also calculated the correlation coefficient between the experimental pK_i or pK_d with ligand MW. The predictions and ranking results are listed in Table 5.

KECSA produces a Pearson's r value of 0.590 and a Kendall τ value of 0.404. Comparison to the training set result (Pearson's $r = 0.610$, $\tau = 0.442$) indicates that KECSA gives robust predictions against an unknown binding affinity dataset. When just using the ligand MW for binding affinity prediction, the Pearson's r drops by 0.128 and the Kendall τ drops by 0.08

Table 5. Statistical Results for KECSA, KECSA LJ, KECSA Entropy, and Ligand MW Correlated with Experimental Binding Affinity

	Pearson's r	Kendall τ
KECSA scoring function	0.590	0.404
LJ potentials in KECSA	0.509	0.352
entropy in KECSA	0.521	0.349
ligand molecular weight	0.381	0.272

Table 6. Statistical Results of KECSA, LISA+, and LISA from Large-Scale Validation Studies[a]

	KECSA			LISA+			LISA		
	test set 1	test set 2	test set 3	test set 1	test set 2	test set 3	test set 1	test set 2	test set 3
correlation coefficient, r	0.553	0.589	0.415		0.572	0.420	0.534	0.542	0.409
RMSE (kcal/mol)	2.46	2.31	2.33		2.81	3.00	2.65	3.06	3.08
Kendall τ	0.401	0.429	0.267		0.419	0.257	0.378	0.397	0.252

[a]Test set 1 contains 1399 complexes from the PDBbind v2010 database. Test set 2 contains 2166 nonmetal complexes from the PDBbind v2011 refined dataset. Test set 3 contains 290 metalloprotein−ligand complexes from the PDBbind v2011 refined dataset.
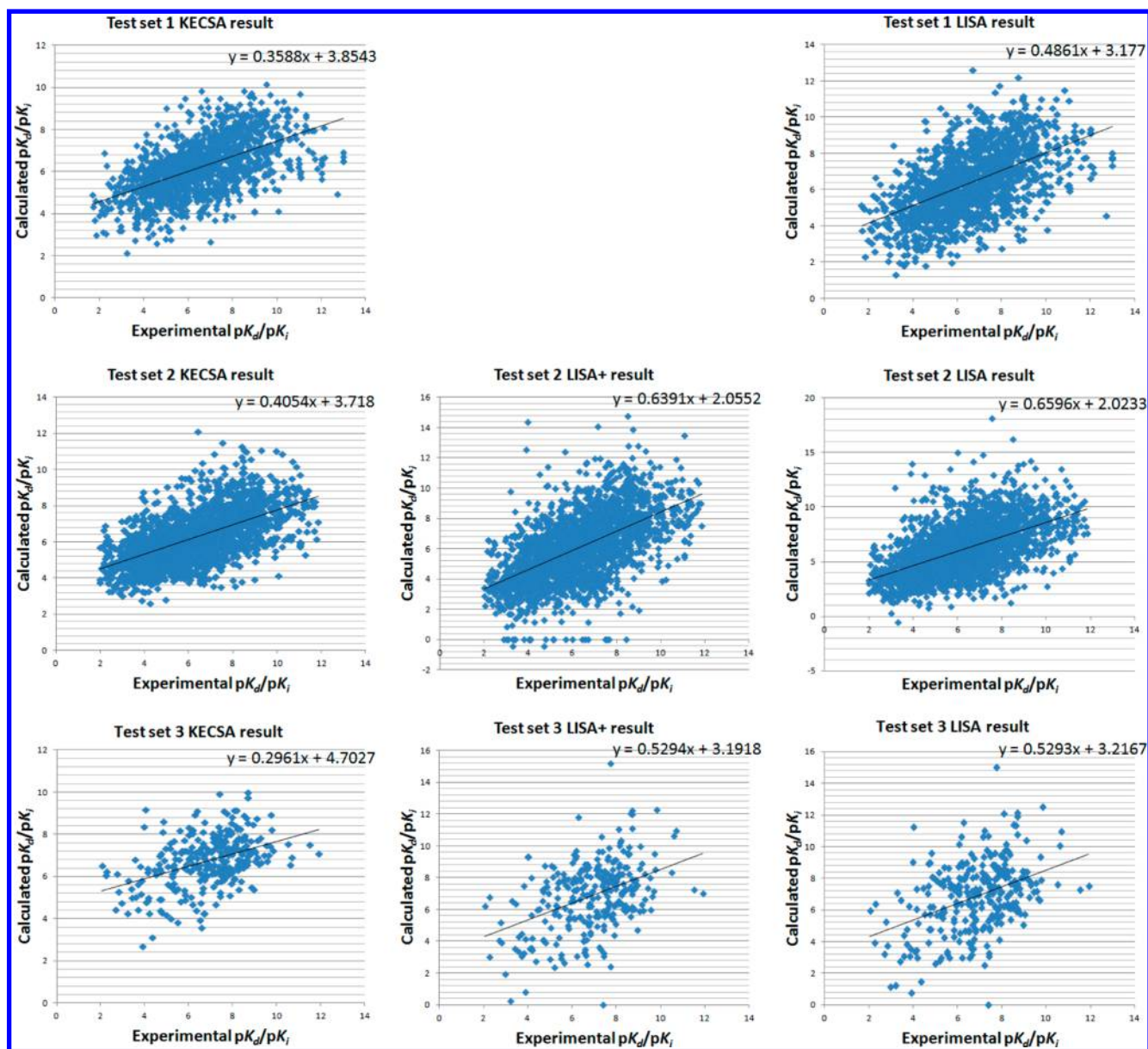

Figure 3. Plot of KECSA, LISA+, and LISA calculated pK_d or pK_i values versus experimental pK_d or pK_i values obtained in validation studies.

when compared to the LJ potential only prediction, while Pearson's r drops by 0.140 and the Kendall τ drops by 0.08 when compared to the entropy term prediction. The drop in prediction is even greater when compared to the full KECSA score function. This result suggests that the KECSA prediction is minimally affected by MW considerations. The LJ potential and entropy only predictions are quite similar, but lower than the full KECSA prediction (see Table 5). None of the two independent parts, enthalpy or entropy, shows a significant

performance over the other, suggesting that both enthalpy and entropy play important roles in the KECSA scoring function. RMSE is not listed for comparison because the LJ potential is generated from a statistical potential while entropy is derived by fitting to pK_d or pK_i values, which results in different scales, making comparison difficult.

II. Validation Benchmark for Comparison with LISA, LISA+, and Other Scoring Methods. KECSA is the second-generation scoring function that we have developed, after

1079

dx.doi.org/10.1021/ci300619x | *J. Chem. Inf. Model.* 2013, 53, 1073−1083

Table 7. Statistical Results of KECSA, Scaled KECSA, LISA+, and LISA from Four Small Test Sets

	KECSA					Scaled KECSA				
	serine protease	endothiapepsin	HIV-1 protease	carbonic anhydrase II	all	serine protease	endothiapepsin	HIV-1 protease	carbonic anhydrase II	all
correlation coefficient, r	0.568	0.441	0.244	0.495	0.591	0.568	0.547	0.245	0.487	0.607
RMSE (kcal/mol)	0.894	1.700	1.678	1.405	1.466	1.299	1.987	1.677	1.478	1.562
Kendall τ	0.423	0.202	0.139	0.246	0.420	0.421	0.067	0.123	0.228	0.390
	LISA+					LISA				
	serine protease	endothiapepsin	HIV-1 protease	carbonic anhydrase II	all	serine protease	endothiapepsin	HIV-1 protease	carbonic anhydrase II	all
correlation coefficient, r	0.692	0.484	0.334	0.427	0.603	0.645	0.496	0.256	0.492	0.586
RMSE	0.970	2.171	1.781	1.814	1.661	1.131	2.880	2.089	1.821	1.884
Kendall τ	0.508	0.353	0.195	0.147	0.407	0.479	0.269	0.118	0.228	0.392
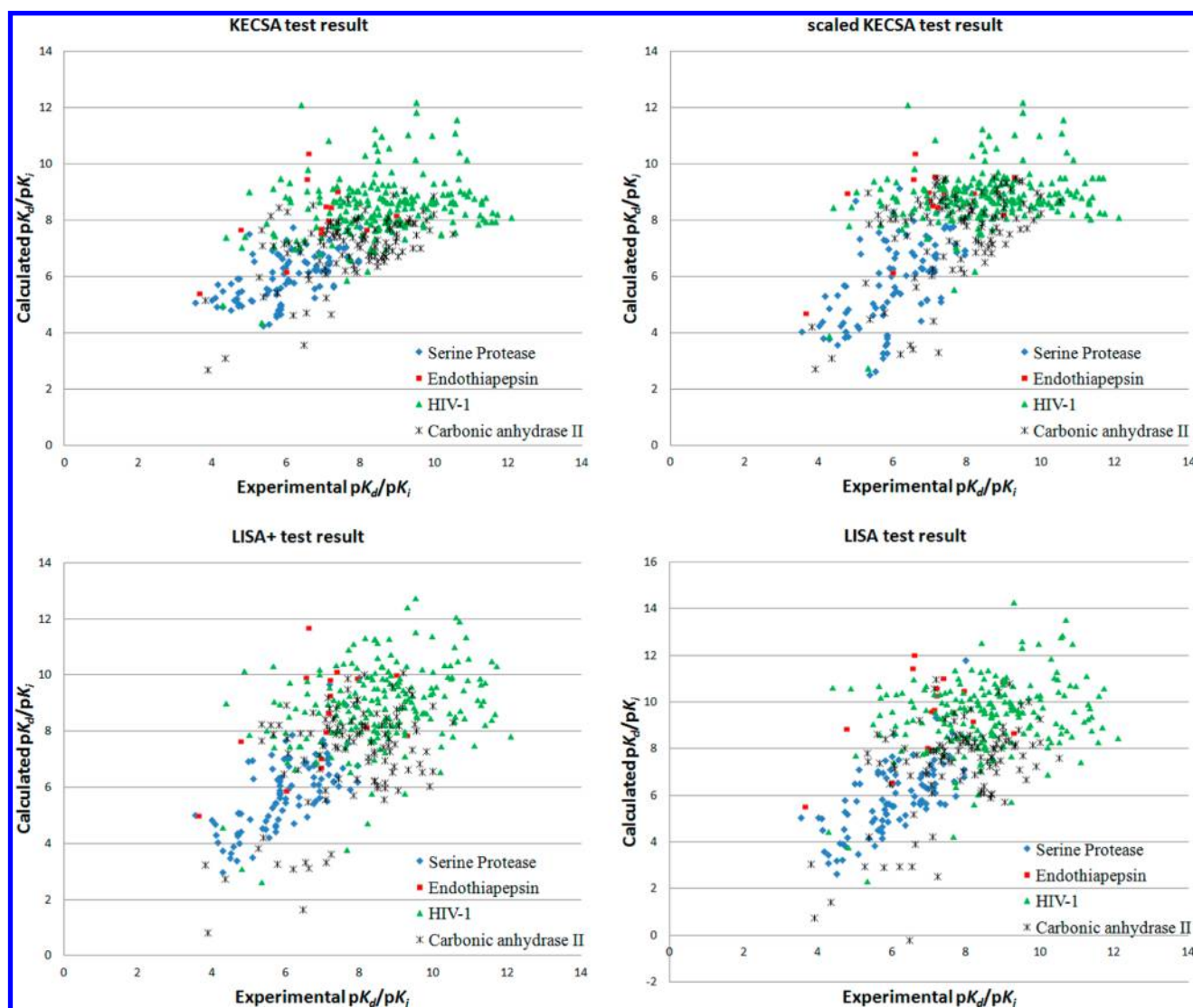
Figure 4. Plot of KECSA, scaled KECSA, LISA+, and LISA calculated pK_d or pK_i values versus experimental pK_d or pK_i values in four small test sets.

LISA[23] and LISA+.[24] The latter two were developed for the fast calculation of protein−ligand binding affinity (pK_d and pK_i), and were successful in the SAMPL3 challenge (first rank for all scoring methods), which was a blind test for docking and scoring methods.[24] Comparisons between KECSA and other scoring methods including LISA and LISA+ are necessary for further understanding its performance. The second validation benchmark consists of two large-scale test sets and four smaller test sets for comparison of KECSA with LISA/LISA+, as well as one small scale test set (Wang's test set[25]) with 100 diverse protein−ligand complexes for comparison of KECSA and several other well-known scoring methods.

First, two large-scale test sets, both with more than 1000 complexes, were introduced to KECSA, LISA, and LISA+. The first test set contained 1399 complexes from the PDBbind v2010 database, which was previously used for LISA validation. KECSA reproduces a Pearson correlation coefficient of $r = 0.553$, an RMSE value of 2.46 kcal/mol, and a Kendall τ parameter of 0.401, while LISA reproduces values of $r = 0.534$, RMSE = 2.65 kcal/mol, and $\tau = 0.378$. LISA+ was trained based on this dataset, so it was excluded from this validation benchmark. A larger test set was applied for all three scoring functions, including 2456 protein−ligand complexes from the PDBbind v2011 refined dataset, of out which 290 complexes had Zn-ligand binding. For those 2166 nonmetal containing complexes, KECSA gets an r value of 0.589, an RMSE value of 2.31 kcal/mol, and a Kendall τ value of 0.429; meanwhile, LISA gets values of $r = 0.542$, RMSE = 3.06 kcal/mol, and $\tau = 0.397$, and LISA+ yields values of $r = 0.572$, RMSE = 2.81 kcal/mol, and $\tau = 0.419$. For those complexes with Zn-ligand binding, KECSA has an r value of 0.415, an RMSE value of 2.33 kcal/mol, and a Kendall τ value of 0.267, while LISA has values of $r = 0.409$, RMSE = 3.08 kcal/mol, and $\tau = 0.252$, and LISA+ has values of $r = 0.420$, RMSE = 3.00 kcal/mol, and $\tau = 0.257$. Calculation and statistical results of KECSA, LISA+, and LISA for all large-scale validation studies are shown in Table 6 and are depicted graphically in Figure 3.

In the large-scale test, KECSA yields a better prediction than our two first-generation scoring functions. It produces better predicted results, based on RMSE, and a more-reliable binding affinity ranking, based on the Kendall τ parameter, compared to the other two scoring methods. LISA+ can compete with KECSA based on correlation coefficient, and even achieves better r in the subset of complexes with Zn-ligand binding. We believe that the improvement of LISA+, compared to LISA, is because the complexes in the training set are categorized based on ligand properties (mass and hydrophobicity) and different models are trained for each category. This proves that a multimodel scheme can improve the predictive ability of empirical scoring functions.

Our validation studies indicate an improvement from LISA to KECSA. Introducing PMF theory for nonbonding interaction modeling shows its advantage of oversimply fitting to binding affinity data. However, the metal−ligand binding prediction remains a challenge for classical-mechanics-based or statistical scoring methods. KECSA improves the binding affinity predicting ability mostly in RMSE for this subgroup of complexes. However, although KECSA shows improvement in both correlation coefficient r and RMSE, predictions in the low and high binding regions are poor. As seen from the linear regression functions in Figure 3, the slopes of LISA and LISA+ generated data versus experimental data are 0.66 and 0.64, respectively, while that for KECSA is 0.41; the intercepts for LISA and LISA+ are 2.02 and 2.06, while that for KECSA result is 3.72. The reason is because 3314 complexes, which comprised 65.3% of the entire training set, are in the midbinding region (pK_d or pK_i values between 4 and 8). Hence, the scoring function tends to overestimate binding affinity of the low-binding region while underestimating that of the high-binding region, if there is no significant decrease or increase in contact number for the protein−ligand complexes from these two regions. We used a scaling procedure to help improve the prediction of binding affinity in the high and low binding regions. The KECSA generated results were fit to a

linear model to reproduce the PDBbind v2011 refined dataset pK_d values. Therefore, we get

$$pK_d = 1.889 \times (pK_d)_{KECSA} - 5.539 \qquad (22)$$

Next, four test sets containing 427 protein−ligand complexes from four protein families were examined. The list of complexes, their families, and binding constants are given in Table 2 in the Supporting Information. Statistical and calculation results are shown in Table 7 and depicted graphically in Figure 4. KECSA improves the RMSE for all test sets, indicating that KECSA makes a more robust prediction, with respect to experimental binding affinity data, than do LISA and LISA+. However, LISA and LISA+ both give a better correlation coefficient r and Kendall τ for the serine protease, endothiapepsin, and HIV-1 protease test sets, showing that they perform better in binding affinity ranking in these small test sets. Results for each test set were carefully examined. The serine protease test set contains many complexes with low-mass ligands, while most ligands are relatively larger in the endothiapepsin test set. Statistical results of the predictions from the three scoring methods are similar in these two test sets: KECSA generates a better RMSE, while LISA and LISA+ yielded both a better correlation coefficient r and Kendall τ. In the serine protease test set, 11 out of 96 protein−ligand complexes had small ligands with molecular mass lower than 200 Da. KECSA prediction overestimates most of their pK_d or pK_i values (see Table 2 in the Supporting Information), while LISA and LISA+, to some degree, underestimate these values. Hence, KECSA decreases the binding affinity differences between these low-binding complexes and other high-binding complexes, while LISA and LISA+ increase these differences. The implication is that LISA and especially LISA+ differentiate the binding affinity values of the complexes better in this test set and give higher r and τ values, but they have worse RMSEs. In the endothiapepsin test set, on the other hand, all complexes have ligands with a molecular mass of >500 Da. LISA and LISA+ overestimated binding affinities with larger errors, compared with KECSA, while distinguishing the complexes better, generating a better linear correlation toward the experimental data. These test results suggest that LISA and LISA+ are more sensitive to ligand mass changes, while KECSA makes more-precise prediction with smaller error, but has difficulty in ranking complexes with similar pK_d or pK_i values. The HIV-1 protease test set is a significant challenge for all three scoring methods. Most of the complexes have high-mass ligands and high binding affinity. Because the ligands in this test set have similar structures, the binding affinity predictions from all three scoring methods are unable to rank these complexes. LISA+ does better in correlation coefficient r and ranking than others, which indicates that training scoring functions for different complex categories based on ligand or binding pocket properties may help scoring methods improve their ability to identify subtle changes in ligand structure. The carbonic anhydrase II test set includes 100 out of 110 complexes with Zn chelation, and contains more polar and charged interactions. KECSA demonstrates better performance in the correlation coefficient r, RMSE, and Kendall τ, highlighting its advantage over LISA and LISA+ with regard to reproducing binding affinity data of complexes with more hydrophilic interactions and metal chelation. For the reproduction of the binding affinity for the four combined test sets, all three scoring methods give a similar correlation coefficient r, while LISA+ has a small advantage. KECSA does better in both RMSE and
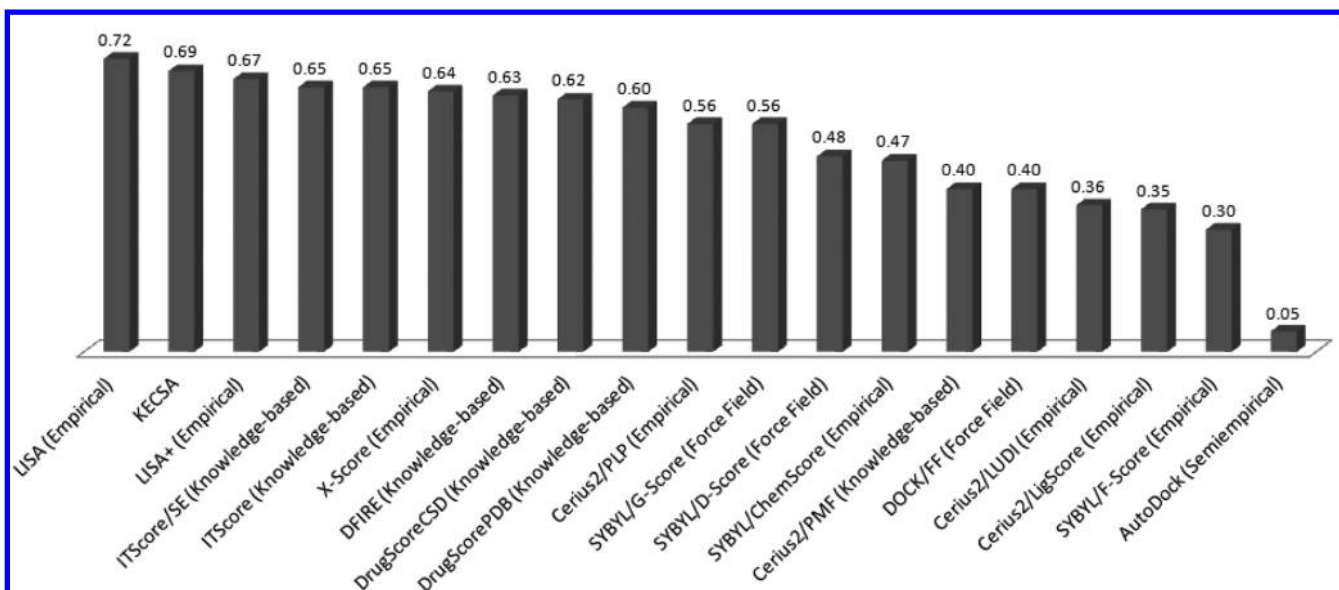
Figure 5. With the test set built by Wang,[25] binding affinity comparison was done for KECSA, LISA, LISA+, and several other well-known scoring functions (ITScore/SE,[18] ITScore,[17] X-Score,[26] DFIRE,[27] DrugScoreCSD,[12] DrugScorePDB,[11] Cerius2/PLP,[28,29] SYBYL/G-Score,[30] SYBYL/D-Score,[31] SYBYL/ChemScore,[32] Cerius2/PMF,[8] DOCK/FF,[31] Cerius2/LUDI,[33,34] Cerius2/LigScore,[35] SYBYL/F-Score,[36] and AutoDock[37]).

Kendall τ. For all four test sets, scaling of the KECSA score does help to improve the slope of calculated data vs experimental data, but does not improve the statistical tests. Overall, KECSA give better RMSE values and better binding affinity ranking of the complexes belonging to different protein families.

For the last test set, we introduced Wang's test set[25] with 100 diverse protein−ligand complexes. The purpose was to compare binding affinity prediction ability of KECSA, not only with LISA and LISA+, but also with other well-known scoring functions. We obtain values of Pearson's $r = 0.69$ and RMSE = 2.25 kcal/mol using KECSA, compared with values of Pearson's $r = 0.72$ and RMSE = 2.32 kcal/mol using LISA, and Pearson's $r = 0.67$ and RMSE = 2.80 kcal/mol using LISA+. This result coincides with the conclusion gained from the second validation benchmark, that, among these three scoring functions, the KECSA prediction has the smallest RMSE value. Pearson correlation coefficients of KECSA, together with other score functions, are presented in Figure 5, showing its performance on this test set.

CONCLUSION AND OUTLOOK

Based on atom pairwise interactions, interaction enthalpy terms in the knowledge-based and empirical combined scoring algorithm (KECSA) method were parametrized by combining potential of mean force (PMF) theory with the Lennard-Jones (LJ) potential, without fitting to any binding affinity data. This procedure parametrizes the LJ potential with neither QM calculations nor binding affinity data, hence lowering the computational expense while improving the prediction accuracy relative to empirical scoring functions. Generally, KECSA improves the binding affinity RMSE, when compared to LISA and LISA+, especially for complexes dominated by polar and charged interactions. With respect to ranking predictions, KECSA better distinguishes complexes in the large-scale test sets. KECSA yields the lowest RMSE values, illustrated by its superior performance in all test sets for this measure of quality. It is less responsive, however, to minor structural changes of the

ligand or binding pocket, reducing its ability to rank complexes from the same or similar protein families. In the KECSA model, the solvent-accessible surface area is introduced to describe the desolvation effect and entropy terms were empirically modeled. Since we have formulated and parametrized the enthalpy component of noncovalent interactions with this alternative method, an interesting possibility is to use similar procedures to build a force field model solely based on experimental structural data. In this way, the desolvation and entropy terms can also be included instead of using empirical models. We believe that more accurate and effective scoring methods can be developed using this concept.

Our group has constructed an in-house docking program where KECSA (as well as LISA and LISA+) is employed as the scoring module in this program. KECSA's ability to score docking poses and distinguish native poses from decoys will be further evaluated and refined in future work using this docking module.

ASSOCIATED CONTENT

Ⓢ Supporting Information

Supporting Information is available, including the Lennard-Jones potential models parameter η values and predicted pK_d or pK_i vs experimental pK_d or pK_i plots for our test sets. This material is available free of charge via the Internet at http://pubs.acs.org.

AUTHOR INFORMATION

Corresponding Author
*E-mail address: merz@qtp.ufl.edu.

Notes
The authors declare no competing financial interest.

■ REFERENCES

(1) Sippl, M. J. Calculation of conformational ensembles from potentials of mean force. *J. Mol. Biol.* **1990**, *213*, 859−883.

(2) Miyazawa, S.; Jernigan, R. L. Estimation of effective interresidue contact energies from protein crystal structures: quasi-chemical approximation. *Macromolecules* **1985**, *18*, 534−552.

(3) Hendlich, M.; Lackner, P.; Weitckus, S.; Floeckner, H.; Froschauer, R.; Gottsbacher, K.; Casari, G.; Sippl, M. J. Identification of native protein folds amongst a large number of incorrect models. The calculation of low energy conformations from potentials of mean force. *J. Mol. Biol.* **1990**, *216*, 167−180.

(4) Jones, D. T.; Taylor, W. R.; Thornton, J. M. A new approach to protein fold recognition. *Nature* **1992**, *358*, 86−89.

(5) Thomas, P. D.; Dill, K. A. An iterative method for extracting energy-like quantities from protein structures. *Proc. Natl. Acad. Sci., U.S.A.* **1996**, *93*, 11628−11633.

(6) Thomas, P. D.; Dill, K. A. Statistical potentials extracted from protein structures: How accurate are they? *J. Mol. Biol.* **1996**, *257*, 457−469.

(7) Lu, H.; Skolnick, J. A Distance-Dependent Atomic Knowledge-Based Potential for Improved Protein Structure Selection. *Proteins: Struct., Funct., Genet.* **2001**, *44*, 223−232.

(8) Muegge, I.; Martin, Y. C. A General and Fast Scoring Function for Protein−Ligand Interactions: A Simplified Potential Approach. *J. Med. Chem.* **1999**, *42*, 791−804.

(9) Muegge, I. A knowledge-based scoring function for protein-ligand interactions: Probing the reference state. *Perspect. Drug Discovery Des.* **2000**, *20*, 99−114.

(10) Muegge, I. Effect of ligand volume correction on PMF scoring. *J. Comput. Chem.* **2001**, *22*, 418−425.

(11) Gohlke, H.; Hendlich, M.; Klebe, G. Knowledge-based scoring function to predict protein−ligand interactions. *J. Mol. Biol.* **2000**, *295*, 337−356.

(12) Velec, H. F. G.; Gohlke, H.; Klebe, G. DrugScore(CSD)-knowledge-based scoring function derived from small molecule crystal data with superior recognition rate of near-native ligand poses and better affinity prediction. *J. Med. Chem.* **2005**, *48* (20), 6296−6303.

(13) DeWitte, R. S.; Shakhnovich, E. I. SMoG: de Novo design method based on simple, fast, and accutate free energy estimate. 1. Methodology and supporting evidence. *J. Am. Chem. Soc.* **1996**, *118*, 11733−11744.

(14) Ishchenko, A. V.; Shakhnovich, E. I. Small molecule growth 2001 (SMoG2001): An improved knowledge-based scoring function for protein-ligand interactions. *J. Med. Chem.* **2002**, *45*, 2770−2780.

(15) Mitchell, J. B. O.; Laskowski, R. A.; Alex, A.; Thornton, J. M. BLEEP—Potential of mean force describing protein−ligand interactions: I. Generating potential. *J. Comput. Chem.* **1999**, *20*, 1165−1176.

(16) Mitchell, J. B. O.; Laskowski, R. A.; Alex, A.; Forster, M. J.; Thornton, J. M. BLEEP—Potential of mean force describing protein−ligand interactions: II. Calculation of binding energies and comparison with experimental data. *J. Comput. Chem.* **1999**, *20* (11), 1177−1185.

(17) Huang, S.-Y.; Zou, X. An iterative knowledge-based scoring function to predict protein−ligand interactions: II. Validation of the scoring function. *J. Comput. Chem.* **2006**, *27*, 1876−1882.

(18) Huang, S.-Y.; Zou, X. Inclusion of Solvation and Entropy in the Knowledge-Based Scoring Function for Protein−Ligand Interactions. *J. Chem. Inf. Model.* **2010**, *50*, 262−273.

(19) Kirkwood, J. G. Statistical Mechanics of fluid Mixtures. *J. Chem. Phys.* **1935**, *3*, 300−313.

(20) Fan, H.; Schneidman-Duhovny, D.; Irwin, J. J.; Dong, G.; Shoichet, B. K.; Sali, A. Statistical potential for modeling and ranking of protein-ligand interactions. *J. Chem. Inf. Model.* **2011**, *51* (12), 3078−3092.

(21) Wang, R.; Fang, X.; Lu, Y.; Wang, S. The PDBbind Database: Collection of Binding Affinities for Protein-Ligand Complexes with KnownThree-Dimensional Structures. *J. Med. Chem.* **2004**, *47*, 2977−2980.

(22) Wang, R.; Fang, X.; Lu, Y.; Yang, C.-Y.; Wang, S. The PDBbind Database: Methodologies and Updates. *J. Med. Chem.* **2005**, *48*, 4111−4119.

(23) Zheng, Z.; Merz, K. M. Ligand Identification Scoring Algorithm (LISA). *J. Chem. Inf. Model.* **2011**, *51*, 1296−1306.

(24) Benson, M. L.; Faver, J. C.; Ucisik, M. N.; Dashti, D. S.; Zheng, Z.; Merz, K. M. Prediction of trypsin/molecular fragment binding affinities by free energy decomposition and empirical scores. *J. Comput.-Aided Mol. Des.* **2012**, *26* (5), 647−659.

(25) Wang, R.; Lu, Y.; Wang, S. Comparative Evaluation of 11 Scoring Functions for Molecular Docking. *J. Med. Chem.* **2003**, *46*, 2287−2303.

(26) Wang, R.; Lai, L.; Wang, S. Further development and validation of empirical scoring functions for structure-based binding affinity prediction. *J. Comput.-Aided Mol. Des.* **2002**, *16*, 11−26.

(27) Zhang, C.; Liu, S.; Zhu, Q.; Zhou, Y. A Knowledge-Based Energy Function for Protein−Ligand, Protein−Protein, and Protein−DNA Complexes. *J. Med. Chem.* **2005**, *48*, 2325−2335.

(28) Gehlhaar, D. K.; Verkhivker, G. M.; Rejto, P. A.; Sherman, C. J.; Fogel, D. B.; Freer, S. T. Molecular recognition of the inhibitor AG-1343 by HIV-1 Protease: Conformationally flexible docking by evolutionary programming. *Chem. Biol.* **1995**, *2*, 317−324.

(29) Gehlhaar, D. K.; Bouzida, D.; Rejto, P. A. In *Rational Drug Design: Novel Methodology and Practical Applications*; Parrill, L., Reddy, M. R., Eds.; American Chemical Society: Washington, DC, 1999; Vol. 719, pp 292−311.

(30) Jones, G.; Willett, P.; Glen, R. C.; Leach, A. R.; Talor, R. Development and validation of a genetic algorithm for flexible docking. *J. Mol. Biol.* **1997**, *267*, 727−748.

(31) Meng, E. C.; Shoichet, B. K.; Kuntz, I. D. Automated docking with grid-based energy approach to macromolecule-ligand interactions. *J. Comput. Chem.* **1992**, *13*, 505−524.

(32) Eldridge, M. D.; Murray, C. W.; Auton, T. R.; Paolini, G. V.; Mee, R. P. Empirical scoring functions: I. The development of a fast empirical scoring function to estimate the binding affinity of ligands in receptor complexes. *J. Comput.-Aided Mol. Des.* **1997**, *11*, 425−445.

(33) Böhm, H. J. The development of a simple empirical scoring function to estimate the binding constant for a protein−ligand complex of known three-dimensional structure. *J. Comput.-Aided Mol. Des.* **1994**, *8*, 243−256.

(34) Böhm, H. J. Prediction of binding constants of ptotein ligands: A fast method for the polarization of hits obtained from de novo design or 3D database search programs. *J. Comput.-Aided Mol. Des.* **1998**, *12*, 309−323.

(35) *CERIUS2 LigandFit User Manual*; Accelrys, Inc.: San Diego, CA, 2000; pp 3−48.

(36) Rarey, M.; Kramer, B.; Lengauer, T.; Klebe, G. A fast flexible docking method using an incremental construction algorithm. *J. Mol. Biol.* **1996**, *261*, 470−489.

(37) Morris, G. M.; Goodsell, D. S.; Halliday, R. S.; Huey, R.; Hart, W. E.; Belew, R. K.; Olson, A. J. Automated docking using a Lamarckian genetic algorithm and an empirical binding free energy function. *J. Comput. Chem.* **1998**, *19*, 1639−1662.